JOURNAL OF CATALYSIS 39, 303–316 (1975)

Deuterium–Hydride Exchange in a Single Catalyst Particle

WILLIAM R. ERNST[1] AND JAMES WEI

University of Delaware, Newark, Delaware 19711

Received October 4, 1974; revised April 15, 1975

The deuterium–neopentane exchange reaction on a single catalyst particle has been used to study the influence of intraparticle diffusion on product distribution. Experimental product distributions agree with those predicted by a two-parameter kinetic model. The parameters Φ and β representing diffusion limitation and desorption limitation, respectively, were varied independently by particle size reduction or catalyst pretreatment with oxygen. Thiele diffusion coefficients obtained from the deuterium–neopentane exchange experiments are about one-half of the Wicke–Kallenbach diffusion coefficients.

I. INTRODUCTION

Intraparticle mass transfer and adsorption–desorption effects play a large role in determining reaction rate and product distribution in heterogeneous catalysts. In a system of many components with coupled complex chemical reactions, theory predicts that a large number of product combinations can be produced by effecting various combinations of mass transfer and desorption limitations. Such a method of "tailoring" a catalyst by modifying its mass transfer and desorption characteristics could be very useful in industrial processes.

The works of Wei and Prater (*1*), Wei (*2,3*) and Mikovsky and Wei (*4*) have provided a technique for analyzing a system of complex chemical reactions when diffusion limitation is present. Kemball (*5*), Bolder *et al.* (*6*) have discussed the effects of desorption limitation on the deuterium–hydride exchange reaction.

Dwyer *et al.* (*7,8*) recently studied the deuterium–neopentane exchange reaction, and experimentally demonstrated the combined effects of mass transfer and desorption limitations on product distribution. They successfully used a two-parameter model based upon the theory that the surface reaction proceeds via a single-step exchange, and that the apparent multistep kinetics results from imposing mass transfer and desorption limitations on the single-step exchange.

The parameter β is the ratio of $\tau_d = 1/k_d$, the length of time that a molecule is adsorbed on the catalyst surface, to $\tau_s = 1/k_s$, the characteristic time for the surface reaction. The term Φ^2 is proportional to the ratio of $\tau_\epsilon = R^2/4D$, the Einstein time that a molecule spends within the catalyst, to $\tau_k = 1/k$, the characteristic time for the intrinsic kinetics.

Dwyer also found that the values of the diffusion coefficients of neopentane from the kinetic data are about one-half of the values obtained by the Wicke–Kallenbach method (*9*). A similar discrepancy was observed by Weisz and Prater (*10*), Balder and Petersen (*11*), Stoll and Brown (*12*), and by Wakao *et al.* (*13*). Explanations that have been offered include catalyst fouling, pore blockage by adsorbed molecules, pore size distributions, surface diffusion and the extrapolation of Wicke–Kallenbach data from ambient to reaction conditions. To arrive at their conclusion,

[1] Present address: Georgia Institute of Technology.

Dwyer *et al.* (*7*) assumed a constant value of diffusivity for neopentane which is independent of concentration, and has a Knudsen dependence on temperature and molecular weight. The first assumption is reasonable in a system with a great excess of D_2, and a fixed concentration for the neopentanes. The second assumption that $D \propto (T/\mathrm{MW})^{1/2}$ is more open to question. A 10% deviation from the assumption of $D \propto (1/\mathrm{MW})^{1/2}$ was observed by Stoll and Brown (*12*) for He–N_2 through γ-alumina. Deviation of greater than 10% was observed for a puzzling single experiment at 26°C by Omata and Brown (*14*). The temperature dependence in $D \propto T^n$ should vary between the Knudsen value of $n = 0.5$ and the bulk value of $n = 1.5$. These values were observed by Omata and Brown except for the puzzling 26°C experiment, where the Knudsen diffusivities for He and N_2 have $n = 0.052$ and 1.1. The discrepancy between kinetic and Wicke–Kallenbach diffusivities observed by Dwyer would increase if $n > 0.5$. An explanation of the discrepancy offered by Dwyer is that large pores may have been created in the catalyst when it was thermally treated. These large pores could have provided a rapid diffusion path that would give large diffusion coefficients in Wicke–Kallenbach measurements, while the small pores contain most of the surface catalytic sites and are more important in the reaction experiments. The kinetic experiments of Dwyer were conducted over a bed of 40 particles, whereas the Wicke–Kallenbach test was conducted on one bead at a time.

Several theoretical models have been developed to predict diffusion rates of binary gases in porous media in the absence of chemical reaction. Horak and Schneider (*15*) recently reviewed and tested the random pore model of Wakao and Smith (*16*), the parallel pore models of Johnson and Stewart (*17*), the work of Rothfeld (*18*) and Scott and Dullien (*19*). Horak and Schneider compared predicted diffusion coefficients with measured values obtained from Wicke–Kallenbach experiments on pellets of compressed aluminum oxide. Weisz and Schwartz (*20*) used two models, one based on a random structure of cylindrical pores, another on a random structure of connecting cells, to predict values of diffusion coefficients for 59 different porous catalysts. Satterfield (*21*) discussed many other studies of this type.

Experiments by Huggill (*22*) in capillaries show that the flow of gases from H_2 to argon and CO_2 follow the $(1/\mathrm{MW})^{1/2}$ relation to within 7%, and that a 5% deviation from Knudsen theory is observed when the radius of the capillary equals the mean free path. Lund and Berman (*23*) found less than 3% deviation from Knudsen theory for the transmission of noble gases in capillaries from 1 to 200 μm diameter. In the transition region where the ratio of tube diameter to mean free path varies from 0.002 to 15, Hanley and Steele (*24*) found a semiquantitative agreement between their data and the limits of Knudsen and Poiseuille.

The present investigation was undertaken to study the effects of desorption and diffusion on the deuterium–neopentane exchange in a single particle of catalyst. An experimental technique was developed to show that β and Φ_1 are independent of each other, so that a change in one parameter does not cause a predictable change in the other.

II. THEORY

A. Desorption and Diffusional Influences on Kinetics of Deuterium–Hydride Exchange

Dwyer *et al.* (*7,8*) developed a two-parameter model for the deuterium–hydride exchange which takes into account the rates of surface exchange, intraparticle diffusion, adsorption and desorption. The derivation of the model is illustrated here for the following reactions:

$$CH_4 \underset{H}{\overset{D}{\rightleftharpoons}} CH_3D \underset{H}{\overset{D}{\rightleftharpoons}} CH_2D_2 \underset{H}{\overset{D}{\rightleftharpoons}} CHD_3 \underset{H}{\overset{D}{\rightleftharpoons}} CD_4. \quad (1)$$

The rate equation for the methane in a closed constant-density system in matrix form is

$$\frac{d}{dt}\vec{a} = -k\,\mathbf{B}\left[I + \frac{\beta}{n}\mathbf{B}\right]^{-1}\vec{a}, \quad (2)$$

where a_i = mole fraction of $CD_i\,H_{n-i}$ in the hydride mixture, n = the number of exchangeable hydrogens in the hydride, k = intrinsic rate constant that includes the dependence on $(D_2 + HD + H_2)$ concentrations, which is many times greater than neopentane concentrations.

$$\mathbf{B} = \begin{bmatrix} 4q & -p & 0 & 0 & 0 \\ -4q & 3q+p & -2p & 0 & 0 \\ 0 & -3q & 2q+2p & -3p & 0 \\ 0 & 0 & -2q & q+3p & -4p \\ 0 & 0 & 0 & -q & 4p \end{bmatrix}, \quad (3)$$

where p = fraction of H in H_2, HD, and D_2; q = fraction of D in H_2, HD, and D_2.

Equation (2) represents a highly coupled system of reversible first order reactions which can be analyzed using the method developed by Wei and Prater (*1*) and Wei (*2,3*). In the presence of diffusion effects, where all the neopentanes share the same constant diffusivity, the rate equation can also be written in the form

$$\frac{d}{dt}\vec{a} = -k\,\mathbf{X}\,\mathbf{\Lambda}''\,\mathbf{X}^{-1}\vec{a}, \quad (4)$$

where $\mathbf{X}$ is the modal or eigenvector matrix of $\mathbf{B}$, and $\mathbf{\Lambda}''$ is the matrix of eigenvalues of the form

$$\lambda_i'' = \lambda_i'\,\eta_i, \quad (5)$$

where

$$\lambda_i' = \frac{i}{1 + i\beta/n}, \quad (6)$$

$$i = 0 \text{ to } n,$$

$$\eta_i = 3\,(\Phi_i \coth \Phi_i - 1)\Phi_i^2, \quad (7)$$

and

$$\Phi_i = R\left(\frac{k\lambda_i'}{D_{ef}}\right)^{1/2}; \quad (8)$$

D_{ef} is the constant effective diffusivity of neopentanes. When $(D_2 + HD + H_2)$ is greatly in excess, their gradients in the catalyst are negligible. The ratio of eigenvalues λ_1'' and λ_n'' is proportional to the average number of D atoms in the initial product, designated by Kemball (*5*) as M. It has the form

$$M = \text{initial}\left[\sum_{i=1}^{n} i a_i \Big/ \sum_{i=1}^{n} a_i\right] = \frac{n\lambda_1''}{\lambda_n''} = \frac{\eta_1}{\eta_n}\left[\frac{n + n\beta}{n + \beta}\right]. \quad (9)$$

To integrate the rate equation, a characteristic species b_i is defined by

$$\vec{b} = \mathbf{X}^{-1}\vec{a} \quad (10)$$

and Eq. (4) is premultiplied by $\mathbf{X}^{-1}$. The resulting equation is

$$\frac{d\vec{b}}{dt} = -\left[k\mathbf{\Lambda}'' + \mathbf{X}^{-1}\frac{d}{dt}(\mathbf{X})\right]\vec{b}, \quad (11)$$

where

$$\mathbf{X}^{-1}\frac{d}{dt}(\mathbf{X}) = \begin{bmatrix} 0 & 0 & 0 & 0 & 0 \\ 4 & 0 & 0 & 0 & 0 \\ 0 & 3 & 0 & 0 & 0 \\ 0 & 0 & 2 & 0 & 0 \\ 0 & 0 & 0 & 1 & 0 \end{bmatrix}\frac{dp}{dt}. \quad (12)$$

The individual equations take the form:

$$\frac{db_0}{dt} = 0, \quad (13)$$

$$\frac{db_1}{dt} = -k\,\lambda_1''\,b_1 - nb_0\frac{dp}{dt}, \quad (14)$$

. . .

. . .

. . .

$$\frac{db_i}{dt} = -k\,\lambda_i''\,b_i - (n + 1 - i)\,b_{i-1}\frac{dp}{dt}. \quad (15)$$

The term p is related to b_1 by the hydrogen balance of the reaction system,

$$p = -np\left(\frac{G+1}{G}\right) + n, \qquad (16)$$

where G = ratio of total H atoms to total D atoms in the reaction system, and

$$\frac{dp}{dt} = \frac{1}{n}\left(\frac{G}{G+1}\right)\frac{db_1}{dt}. \qquad (17)$$

The solution to Eq. 13 is:

$$b_0(t) = 1 \text{ for all } t. \qquad (19)$$

The solution to Eq. (14) is

$$b_1(t) = b_1(0) \exp\left[-k\lambda_1''(1+G)t\right]. \qquad (20)$$

The remaining Eqs. (15) are solved recursively. Solution to the general $b_i(t)$ equation is a sum of i exponential terms. It can easily be shown that $k\lambda_i''$ is a function of $k\lambda_1''$ and Φ_1; therefore each of the characteristic species b_i will be function of $k\lambda_1''$, t and two parameters β and Φ_1.

B. Effect of Catalyst Pore Size Distribution

There are many reasons why the Wicke–Kallenbach (WK) diffusivity, measured in the absence of reaction, should be up to 50% greater than the kinetic diffusivity obtained from an examination of the effectiveness factor, and Thiele modulus. The presence of large cracks would greatly increase the WK diffusivity, with negligible effect on the kinetic diffusivity. The presence of many very small diameter deadend pores would, on the other hand, decrease the average kinetic diffusivity with negligible effect on the WK diffusivity. Surface diffusion does not explain the difference unless it is very great for H_2 at room temperature and vanishes for neopentane at reaction temperatures. The concentration dependency of diffusivity is unimportant, since the concentration of neopentanes are fixed. Variations of the assumption $D \propto (T/\mathrm{MW})^{1/2}$ to higher powers of T only make the differences greater.

A possible explanation of the difference between the WK and kinetic diffusivities is in the pore size distribution in the catalyst. No model has been developed that is totally satisfactory. The simple parallel pore model was adopted here, which is reasonable for unimodal pore size distributions with narrow dispersions. A model will be developed here for a flat plate geometry, with nonintersecting pores of uniform diameter. The pores of each diameter will develop its own distinctive concentration gradient. The effects computed here represent an upper bound to the influence of pore size distribution, as the intersection of pores of different sizes would lead to less distinctions between pores.

1. Diffusion Without Reaction

Consider a flat plate of width $2L$ containing parallel cylindrical pores. During a Wicke–Kallenbach experiment, the total diffusive flux of gas A through the pores is the integrated rate of diffusion through all the pores divided by the total cross-sectional area of the plate:

$$\frac{\text{flux}}{\text{area}} = \frac{\int_0^\infty D(r)\,f(r)\,dr}{\int_0^\infty f(r)\,dr} \cdot \frac{\Delta C}{2L}\,\theta, \qquad (21)$$

where r pore radius
$f(r)$ pore volume distribution function, $\int_0^\infty f(r)\,dr = 1$
$D(r)$ diffusion coefficient in a pore of radius r
θ pore volume fraction in catalyst
ΔC the difference in concentration of gas A across the width of the plate $2L$.

The Wicke-Kallenbach diffusion coefficient of the plate determined by this method is

$$D_{WK} = \frac{\int_0^\infty D(r)\, f(r)\, dr}{\int_0^\infty f(r)\, dr}\,\theta. \qquad (22)$$

In terms of volume fractions, Eq. (22) can be written as a sum of terms (*20*):

$$D_{WK} = \sum_i D_i f_i \theta. \qquad (23)$$

2. Diffusion with Reaction

When the catalyst is distributed uniformly over the surfaces, an overall effectiveness factor for the catalyst is (*25,26*):

$$\bar{\eta} = \frac{\int_0^\infty \{[\eta(r)\, f(r)\, dr]/r\}}{\int_0^\infty \{[f(r)\, dr]/r\}}, \qquad (24)$$

where $\eta(r)$ effectiveness factor for a pore of radius r, $= \tanh \Phi(r)/\Phi(r)$

$\Phi(r)$ Thiele modulus for a pore of radius r, $= L\left(\frac{2k_s}{r\,D(r)}\right)^{1/2}$

k_s reaction rate constant per surface area

The overall effectiveness factor η can be related to an experimentally determined Thiele modulus by the equation

$$\bar{\eta} = \frac{\tanh \bar{\Phi}}{\bar{\Phi}}, \qquad (25)$$

where

$$\bar{\Phi} = L\left(\frac{k}{D_{Th}}\right)^{1/2}, \qquad (26)$$

k effective volumetric rate constant, $= 2k_s\,\theta\,\Sigma\, f_i/r_i$

θ void fraction in catalyst

D_{Th} effective Thiele diffusion coefficient for the catalyst.

For computational purposes Eq. (24) can be converted to a sum:

$$\bar{\eta} = \frac{\tanh \bar{\Phi}}{\bar{\Phi}} = \frac{\Sigma_i\, (\tanh \phi_i/\phi_i)(f_i/r_i)}{\Sigma_i\, (f_i/r_i)}, \qquad (27)$$

where r_i pore radius

f_i volume fraction of pores with radius r_i

D_i diffusion coefficient for a pore with radius $r_i = [D_{Knudsen}^{-1} + D_{bulk}^{-1}]^{-1}$.

3. Comparison of Diffusion Coefficients

Equation (26) shows that the overall diffusion coefficient D_{Th} is a function of the pore distribution and $\bar{\Phi}$; whereas in Eq. (23), D_{WK} is a function of pore distribution only. Consider the case where $\phi > 3$, η is reduced to $1/\phi$; when Knudsen diffusion dominated, $D(r) = \epsilon r$ where the parameter ϵ depends on temperature and molecular weight. Equation (23) reduces to

$$D_{WK} = \epsilon\,\theta \sum_i r_i f_i, \qquad (28)$$

while Eq. (27) gives

$$\bar{\eta} = \frac{\epsilon^{1/2}}{L(2k_s)^{1/2}} \cdot \frac{1}{\Sigma_i (f_i/r_i)}, \qquad (29)$$

$$D_{Th} = k(\bar{\eta}L)^2 = \frac{\epsilon\theta}{\Sigma_i (f_i/r_i)}.$$

Therefore the ratio of diffusivities becomes

$$\rho = \frac{D_{Th}}{D_{WK}} = \frac{1}{\Sigma_i (f_i/r_i)\ \Sigma_i r_i f_i}. \qquad (30)$$

If the number distribution of pores were used instead, the result would have been

$$\rho = \frac{D_{Th}}{D_{WK}} = \frac{m_2^2}{m_1 m_3}, \qquad (31)$$

where m_i = the ith moment of the pore radius number distribution $= \int_0^\infty r^i\, N(r)\, dr$.

It has been shown (*20*) that the value of ρ is always less than 1. When the value of $\Phi < 3$, and when gaseous diffusion dominates, the value of ρ would be close to 1. The value of ρ is thus between 1 and $(\Sigma(f_i/r_i)\ \Sigma f_i r_i)^{-1}$. When the pore volume distribution follow a log-normal distribution

$$f(r) = \frac{1}{\sigma r (2\pi)^{1/2}}\, e^{-[(\ln r - m)/\sigma]^2 (1/2)}$$

the moments of $f(r)$ are

$$\int_0^\infty r^j f(r)\, dr = \exp(jm + j^2\sigma^2/2),$$

so that

$$\rho_{\min} = [\exp(m + \sigma^2/2) \times \exp(-m + \sigma^2/2)]^{-1} = \exp(-\sigma^2).$$

The value of σ is often tedious to compute from a given volume distribution. A convenient estimate of σ is available by measuring $r_{0.1}$, the pore radius that is larger than 10% of the pores by volume, and $r_{0.9}$, the pore radius that is larger than 90% of the pores by volume. The value of σ is given by

$$\sigma = 0.3891 \ln (r_{0.9}/r_{0.1}).$$

$r_{0.9}/r_{0.1}$	σ	$\rho_{\min}$
1	0	1.000
1.5	0.158	0.976
2	0.270	0.930
4	0.539	0.747
7	0.757	0.584
10	0.896	0.448
15	1.054	0.329
20	1.166	0.257

III. EXPERIMENTAL METHODS

The equipment for the deuterium–neopentane exchange consists of a reactor shown in Fig. 1 and a mass spectrometer for analysis. The reactor is a 241 cm^3 spherical flask with openings for charging catalysts and reaction gases, and for extracting samples. A removable porous platform designed to support a single catalyst particle extends into the center of the reactor through an opening in the side. A sample leg, a piece of hollow glass tubing with 0.7 cm^3 of internal volume isolated by two stopcocks, extends out from the side of the reactor. It is used to transfer small increments of gases from the reactor to a sample bulb which could be attached to the end of the sample leg.

CP Grade deuterium at 99.5% purity and Research Grade neopentane at 99.9% purity were used. The deuterium was further purified by passing it through a Deoxo unit and through a liquid nitrogen cold trap. Each catalyst was prepared by soaking a solid catalyst support in a solution containing a palladium salt, followed by drying and reduction. The supports, microporous spheres made of 90% silica and 10% alumina ranging in diameter from 0.3 to 0.4 cm, were supplied by Mobil Research and Development Corp.

Catalyst C was prepared by vacuum impregnating a support bead with a solution of $PdCl_2$ in aqueous HCl for 36 hr. After the soaking, it was towel dried, and then dried in a muffle furnace for 1 hr at 110°C.

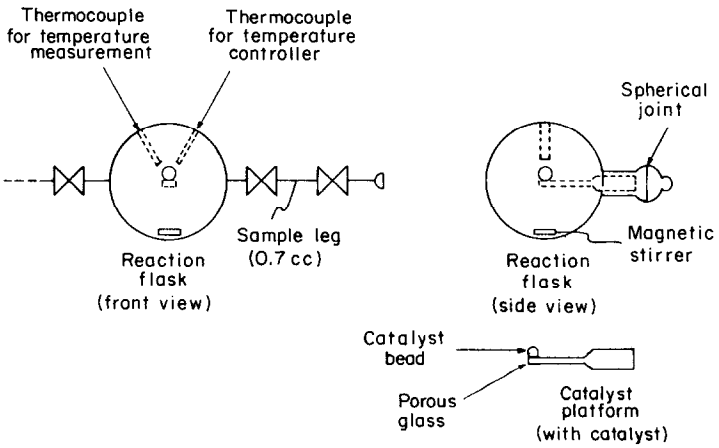

FIG. 1. Deuterium–neopentane exchange reactor.

It was reduced by passing a stream of pure hydrogen over it for 1 hr at 250°C, then cooling to room temperature in flowing nitrogen. It was then heated in oxygen at 350°C for 16 hr. [A previous paper (*27*) reported that oxygen pretreatment greatly reduced the β parameter found for the deuterium–neopentane exchange over supported palladium].

Soaking beads in the aqueous acid solution caused cracks and breakage in many attempts to prepare catalysts. Presoaking the beads in acetone prior to soaking them in the aqueous acid solution reduced the frequency of breakage; however, the breakage was minimized by eliminating the aqueous solution and using a solution of dichlorobisbenzo-nitrile Pd (II) in methylene chloride to impregnate the beads. Drying and reduction steps were as before.

TABLE 1
EXPERIMENTAL CONDITIONS

Runs[a]	T (°C)	$P_{D_2}/P_{C_5H_{12}}$	Catalyst			
			Geometry	No. of pieces	Wt (g)	Pretreatment with O_2
A1	179	19.8	Whole bead	1	0.0215	No
A2	174	20.1	Whole bead	1	0.0215	No
A3	161	19.5	Whole bead	1	0.0215	No
A4	172	19.2	Whole bead	1	0.0215	No
A5	182	20.0	Whole bead	1	0.0215	Yes
B1	154	19.4	Whole bead	1	0.0345	No
B2	178	19.8	Whole bead	1	0.0345	No
B3	200	19.8	Whole bead	1	0.0345	No
B4	192	19.6	Whole bead	1	0.0345	No
B5	203	19.7	1/2 Bead	2	0.0345	No
B6	204	19.5	1/4 Bead	2	0.0170	No
B7	204	19.6	~1/12 Bead	5	0.0167	No
B8	313	20.0	~1/12 Bead	5	0.0167	No
B9	243	19.9	~1/12 Bead	5	0.0167	No
B10	278	20.1	~1/12 Bead	5	0.0167	No
B11	264	19.1	1/2 Bead	1	0.0176	Yes
B12	266	19.4	1/2 Bead	1	0.0176	Yes
B13	266	20.0	1/2 Bead	1	0.0176	Yes[b]
B14	259	20.2	1/2 Bead	1	0.0176	Yes[b]
B15	268	20.3	1/2 Bead	1	0.0176	Yes[b]
C1	198	18.9	Whole bead	1	0.0358	Yes
C2	177	23.1	Whole bead	1	0.0358	Yes
C3	223	19.0	Whole bead	1	0.0358	Yes
C4	193	18.9	Whole bead	1	0.0358	Yes
C5	223	18.3	Whole bead	1	0.0358	Yes
C6	285	19.8	60–80 mesh	Crushed	0.0131	Yes
C7	255	20.4	60–80 mesh	Crushed	0.0097	Yes
C8	303	19.1	60–80 mesh	Crushed	0.0114	Yes[c]

[a] Catalyst A was used in runs A1–A5; catalyst B was used in runs B1–B15; and catalyst C was used in runs C1–C8.

[b] O_2 treatment followed by exposure of the catalyst to neopentane at 270°C for about 2 hr prior to the experiment.

[c] O_2 treatment followed by H_2 treatment of the catalyst for 9 hr at 350°C.

Catalysts A and B were prepared in this manner. No oxygen pretreatment was employed.

After a bead had been used in an exchange experiment, and before it was used in each succeeding experiment, it was reduced in flowing hydrogen at 225–350°C and then given an additional pretreatment with oxygen or neopentane, given no additional pretreatment, or reduced in size by cutting or crushing. Table 1 lists all of the experimental conditions, the catalyst geometry and the pretreatment of the catalyst for each experiment. All experiments are at 1 atm pressure. The ratio of D_2/neopentane is 19:1.

The study of a single catalyst particle required that the scale of equipment and the volumes of gas used in each experiment be small. This required that each gas sample volume also be small. The limitation in the sensitivity of analytical equipment to very small samples required that special handling be given to the samples. Samples taken from the reactor via the sample leg were expanded into evacuated 25 cm^3 sample bulbs and were stored in liquid nitrogen until they were analyzed. Analysis was performed using a CEC 21-110B mass spectrometer. Deuterium was first removed from the samples by submerging the sample bulb in liquid nitrogen to freeze the neopentane, and then pumping off the deuterium. Next the bulb was removed from the liquid nitrogen, allowed to heat up to room temperature, and then attached to a hollow probe which extended into the electron bombardment source of the mass spectrometer. A metering valve on the hollow probe was adjusted to maintain a sample pressure of about 2×10^{-6} Torr in the electron bombardment source. These extreme measures are necessary in order to analyze the gas, otherwise there would be losses and errors in gas analysis.

Since the parent ion for the neopentane is of low intensity in the mass spectrometer, the products were analyzed in terms of the *t*-butyl fragments. This method is based on an assumption also used by Dwyer *et al.* (*7*) and Kemball (*5*) that the hydrogen and deuterium atoms are randomly distributed in $C_5D_iH_{12-i}$, and that removal of the CD_jH_{3-j} group occurs at random. Thus the product distribution for each sample included 10 species, C_4H_9 through C_4D_9.

Raw mass spectrometer data were converted to product distributions by making corrections for natural isotope abundances and fragmentation of the *t*-butyl ions.

Values of Φ_1 and β which minimized the difference between experimental and predicted product concentrations were found by first assuming values for the two parameters, Φ_1 and β, then calculating a $\vec{b}$ vector at the mean deuteration of each experimental sample. The product concentration vectors were calculated by applying the formula $\vec{a} = \mathbf{X}\,(\mathrm{p})\,\vec{b}$. A residue function, defined by

$$\Psi = \left(\sum^{n} \sum_{i=0}^{9} (a_{i,\mathrm{expt}} - a_{i,\mathrm{calc}})^2 \right)^{1/2}$$

(where N = the total number of samples in the experiment) was computed. The above sequence of calculations was repeated for different combinations of Φ_1 and β until parameter values which produced the best fit between experiment and model (i.e., minimum Ψ) were found. D_{WK} values were measured for each catalyst used in the reaction experiments using a H_2–N_2 system (*28*).

IV. RESULTS AND DISCUSSION

Table 2 presents the parameter k, Φ_1, β, M, and Ψ for all of the experiments. Figures 2, 3 and 4 illustrate the comparison between experimental values of the characteristic species and the values predicted by the two-parameter model (solid lines) for runs A4, B3, and C7. The broken lines represent values of the characteristic species which correspond to a binominal

TABLE 2
EXPERIMENT PARAMETERS

Run	T (°C)	k (sec^{-1})	β	Φ_1 (at T)	M	$\psi \times 10^3$)
A1	179	2.174	1.55	8.9	3.89	7.76
A2	174	0.248	0.92	3.1	2.96	4.79
A3	161	0.091	0.47	1.8	2.17	5.05
A4	172	0.274	1.09	3.5	3.16	4.39
A5	182	0.415	0.81	3.6	3.01	6.78
B1	154	0.250	0.41	2.0	2.23	7.99
B2	178	0.815	1.14	4.0	3.29	5.04
B3	200	2.143	1.50	9.0	3.80	6.98
B4	192	0.896	1.11	5.1	3.41	7.03
B5	203	0.343	0.57	2.0	2.34	4.19
B6	204	0.283	0.39	1.6	2.01	5.13
B7	204	0.176	0.39	0.8	1.53	6.05
B8	313	20.600	2.08	19.0	4.31	8.43
B9	243	0.430	0.40	1.3	1.84	6.19
B10	278	5.840	1.92	5.1	3.87	10.10
B11	264	1.820	0.41	4.9	2.91	6.68
B12	266	17.500	1.47	26.6	4.02	9.94
B13	266	1.340	1.30	3.4	3.26	5.39
B14	259	2.120	1.66	4.8	3.70	5.18
B15	268	0.960	0.90	2.9	2.89	4.87
C1	198	1.240	1.39	5.4	3.61	6.69
C2	177	0.105	0.22	1.5	1.84	5.85
C3	223	0.297	0.26	2.6	2.36	4.11
C4	193	0.0235	0.07	0.7	1.27	3.83
C5	223	0.483	0.53	3.5	2.80	5.56
C6	285	0.280	0.00	0.8	1.28	1.51
C7	255	0.019	0.02	0.1	1.02	1.34
C8	303	0.159	0.03	0.8	1.30	2.01

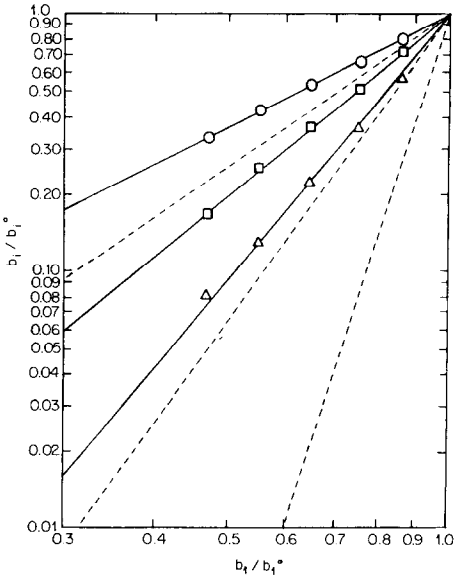

FIG. 3. Logarithmic relationship between characteristic species for Expt B3 (legend as for Fig. 2).

distribution. The deviation of the experimental points from the broken lines illustrated the deviation of the product distribution away from binomial because of diffusion and desorption limitations. Figures 5, 6 and 7 compare the experimental and predicted values of hydride percentage for these same runs. Due to the smaller

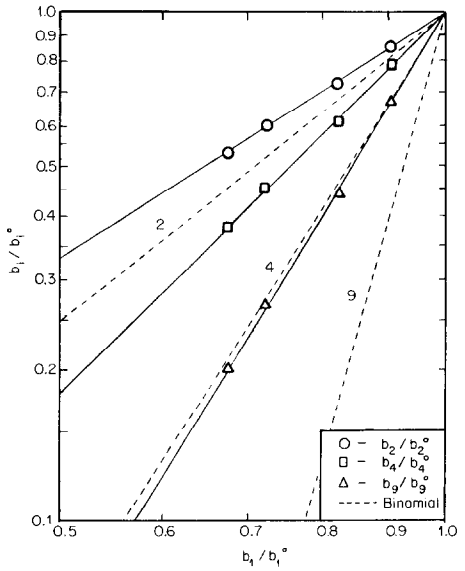

FIG. 2. Logarithmic relationship between characteristic species for Expt A4.

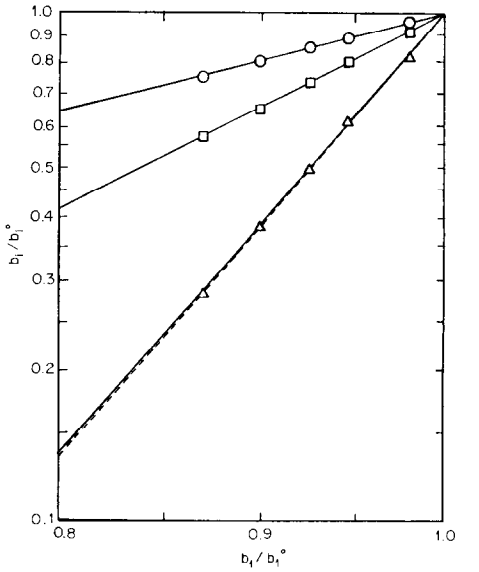

FIG. 4. Logarithmic relationship between characteristic species for Expt C7 (legend as for Fig. 2).

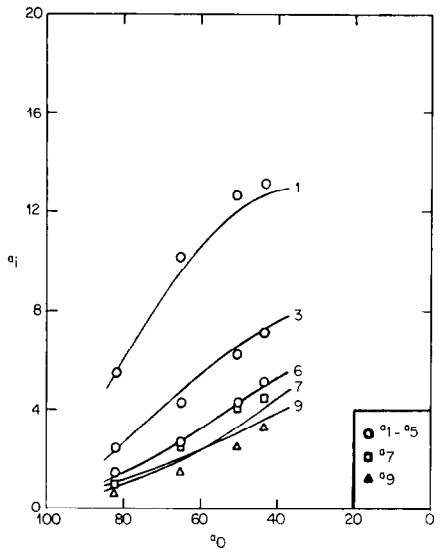

FIG. 5. Distribution of species Expt A4.

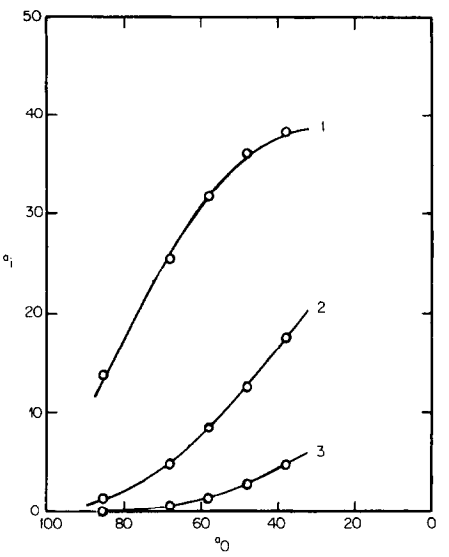

FIG. 7. Distribution of species Expt C7.

scale of equipment and the resulting analytical problems, the average deviation in fit in this study is $\Psi = 5.67 \times (10^{-3})$ compared to $2.23 \times (10^{-3})$ for the previous study (*7*). The agreements are quite good considering the difficulties of single bead experiments.

Figures 4 and 7 show good agreement between experimental data and the two-parameter model. Experiment C7 which was run on a crushed oxygen-pretreated catalyst, gives strong indication that a single-step exchange is the true kinetic mechanism at 255°C. The solid lines in Fig. 4 for the two-parameter model almost completely coincide with the broken lines representing a binomial product distribution. Because of the crushing and oxygen pretreatment, the diffusion and desorption limitations were eliminated and the single-step mechanism was exposed. Parameter values were $\beta = 0.02$ and $\Phi = 0.1$.

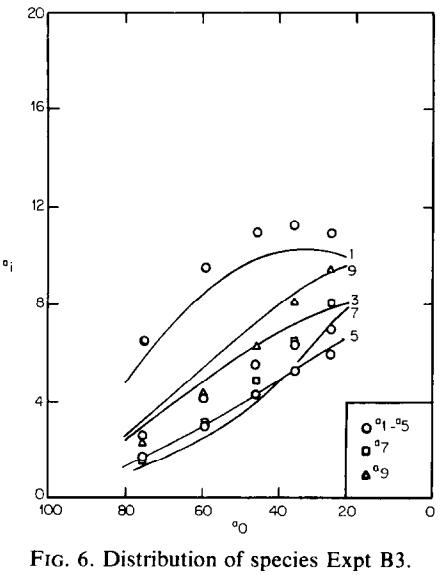

FIG. 6. Distribution of species Expt B3.

One of the objectives of this investigation was to test the two-parameter model over a wide range of conditions to determine whether β and Φ_1 were independent parameters with the physical significance attributed to them by the assumed model. In theory, if these parameters are independent, it should be possible to vary either parameter while holding the other one constant. The variables that affect Φ_1 are temperature and particle size; whereas those that affect β are temperature and catalyst pretreatment. It is difficult to hold one parameter constant while varying the other, and simultaneously maintaining the same level of activity in consecutive runs. After either oxygen pretreatment or catalyst size reduction was performed, a no-

ticeable reduction in intrinsic activity occurred. The reduction is probably the result of impurities introduced during catalyst modification. Experiments B6 and B7 were successful attempts at varying Φ_1 from 0.8 to 1.6 while β remains at 0.39 (see Table 2). This change in Φ_1 was effected by reducing the particle size in Expt B7, while both experiments remain at the same temperature.

Comparisons of B1 with B5 and B4 with B10 illustrate successful attempts at changing β while holding Φ_1 constant. The method used was to reduce particle size and to raise reaction temperature. Attempts at reducing β independent of Φ_1 by oxygen pretreatment were unsuccessful because of the change in catalyst activity which resulted. Instead of comparing individual experiments at the same level of activity, it is easier to compare families of experiments over a range of activities. The act of catalyst size reduction should greatly reduce the Thiele modulus Φ_1, but should have no effect on β. The effect of size reduction on Φ_1 for catalyst B is shown in Fig. 8. The parameter $\Phi_1^{2,*}$ is based on a diffusion coefficient, adjusted to 450°K by the square root of T, and should be a linear function of $k\lambda_1'$. The slope should be proportional to the square of effective catalyst diameter. Calculated geometric factors agree well with experimental values obtained from the slopes. The absence of size reduction effect on β is shown in Fig. 9. Oxygen pretreatment reduces the value of β, but neopentane treatment almost restores the full value of β. This effect is also shown in Fig. 10, where the solid line represents nonoxygen treated, whole, catalyst B bead. Size reduction shifted the β versus $\Phi_1^{2,*}/\lambda_1'$ relationship to the left of the solid line. Oxygen pretreatment shifted the data below the solid line. A similar graphical analysis was made on catalyst A. Oxygen pretreatment caused only a slight change in $\Phi_1^{2,*}$ but a large reduction in β.

Another purpose of this investigation was to obtain values for the effective diffusion coefficient for each single catalyst bead from the $\Phi_1^{2,*}$ versus $k\lambda_1'$ relationship. The values in Table 3, obtained from the slopes of the straight lines in

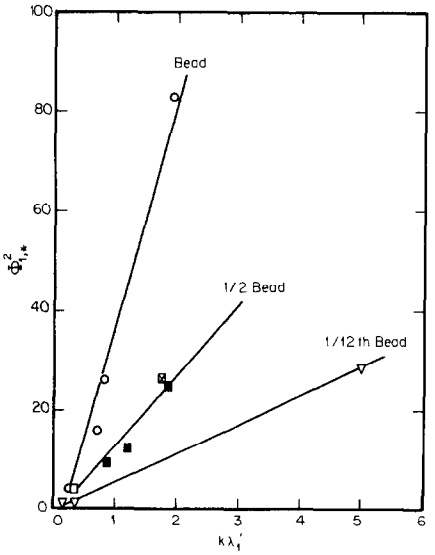

FIG. 8. Relationship between Thiele modulus and $k\lambda_1'$ for catalyst B; effect of particle size (legend as for Fig. 9).

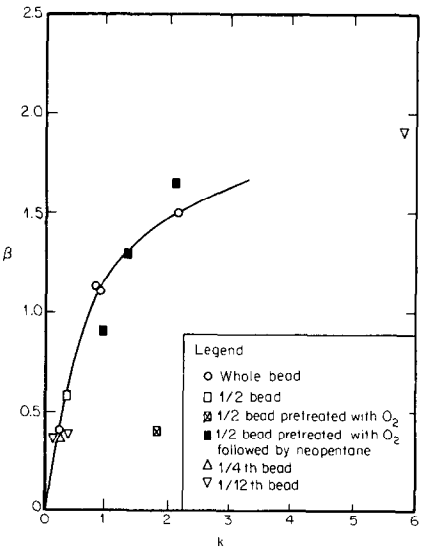

FIG. 9. Relationship between desorption parameter and rate constant for catalyst B; effect of catalyst pretreatment.

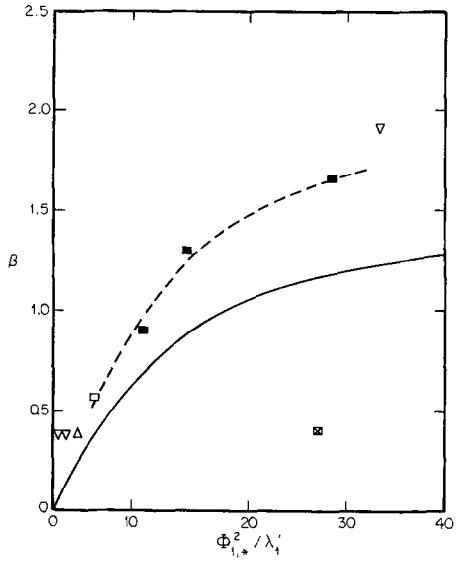

FIG. 10. Relationship between diffusion and desorption parameters for catalyst B; effect of catalyst pretreatment and size reduction (legend as for Fig. 9).

Fig. 8 and similar plots for catalyst A and C were compared with values from the Wicke–Kallenbach experiments. The Thiele diffusion coefficients measured in the kinetic experiments are about one-half of those measured in the Wicke–Kallenbach experiments. The findings are in accordance with previous work for a bed of beads (*7*).

Dwyer suggested that the difference in the diffusion coefficients might have been caused by large cracks produced during thermal treatment of the catalyst. Since the outer portion of the spherical particles would receive the most severe treatment, larger pores might have been formed. The presence of larger pores would increase the rate of diffusion through a bead in the Wicke–Kallenbach experiment, but would not greatly increase the measured rate of diffusion in a kinetic experiment. Most of the catalyst surface area is in the small pores.

The small volume of the catalysts precluded the use of mercury penetration to measure pore distribution of the single catalyst particles. Mobil Research and Development however provided the average pore distributions of the three batches of silica–alumina supports from which the catalyst particles for this study were drawn. Table 4 shows the distribution for these supports. All show less than 2% in the larger pore sizes, $r = 100$–500 Å. The catalysts used in this study may have higher percentages of the larger pores which were created during impregnation with the palladium salt solution. The evidence of catalyst breakage during the impregnation phase, lends support to this hypothesis.

To determine the effect of the pore distribution in the catalysts, the values of D_{Th}/D_{WK} were estimated using the pore distributions from Table 4 and the parallel pore model for a flat plate from Sect. II. The case of high diffusion limitation (Φ very large) was calculated using Eq. (30). Table 4 shows that all of the calculated diffusivity ratios are less than 1; however none are as low as the experimental values in Table 3.

A relatively small percentage of larger

TABLE 3
EXPERIMENTAL EFFECTIVE DIFFUSION COEFFICIENTS

Catalyst	D_{H_2} @ 25°C from H_2–N_2 expts (10^{-3} cm²/sec)	$D_{C_5H_{12}}$ @ 178°C from H_2–N_2 expts (10^{-3} cm²/sec)	$D_{C_5H_{12}}$ @ 178°C from deuterium exchange (10^{-3} cm²/sec)	Ratio of D from deuterium exchange to D from H_2–N_2 expts
A	4.60	0.95	0.59	0.62
B	9.51	1.96	0.82	0.42
C	11.44	2.36	1.13	0.48

TABLE 4
PORE VOLUME DISTRIBUTION FOR SILICA–ALUMINA CATALYST SUPPORTS BY MERCURY PENETRATION[a]

Pore radius (Å)	Pore vol (%) No.: G945	38381[b]	38382
0–15	—	—	—
15–17.5	62.30	1.11	2.17
17.5–20	22.95	1.40	0.54
20–25	3.28	3.47	2.17
25–30	3.28	7.81	2.71
30–35	1.64	20.78	4.62
35–40		56.09	13.86
40–45	2.62	6.16	31.80
45–50		0.14	31.26
50–100	2.29	1.30	9.52
100–500	1.64	1.74	1.35
Void fractions	0.36	0.42	0.43
D_{Th}/D_{WK} [calcd using Eq. (30)]	0.80	0.90	0.89

[a] Tests were run at Mobil Research and Development. The three catalysts listed were batches of silica–alumina beads which had undergone various steam treatments. For this study catalyst A was taken from Batch No. G945, Catalyst B from Batch No. 38381, and Catalyst C from Batch No. 38382.

[b] These figures represent the average of two pore size distribution measurements made on this catalyst.

pores would greatly change D_{Th}/D_{WK}. For example if 4% of 800 Å pores were added to the pore distribution of support No. G945 from Table 4, the calculated D_{Th}/D_{WK} value would equal 0.51.

The sensitivity of parameters was investigated, to determine how a small error in the measurement of one of the parameters would affect the accuracy of the other parameter. Of particular interest was the effect of small changes in β on the accuracy of the function $1/\Phi_1^2$,* because this function is directly proportional to the effective diffusion coefficient.

Sensitivity, S, which was determined for each experiment, was defined by the following equation:

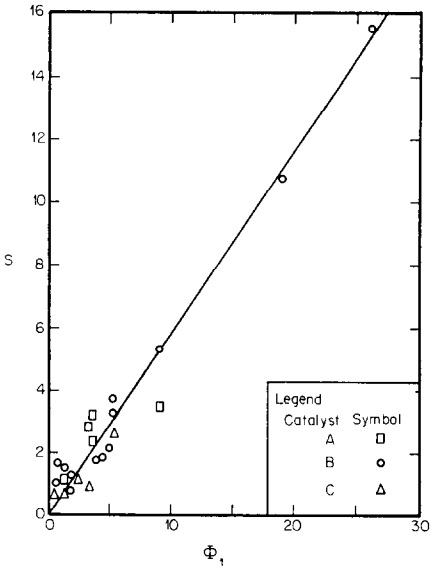

FIG. 11. Sensitivity of parameters.

$$S = \frac{\Delta(1/\Phi_1^2)}{(1/\Phi_1^2)} \left(\frac{\beta}{\Delta\beta}\right),$$

where β and Φ_1 are the parameter values which produce the best fit between experimental data and the two parameter model. The value $\Delta(1/\Phi_1^2)$ was determined by perturbing the value of β by an amount $\Delta\beta$ and then applying the two parameter model to determine the value Φ_1 which produced the best fit between experiment and theory. The value of $\Delta(1/\Phi_1^2)$ was defined by the equation:

$$\Delta(1/\Phi_1^2) = 1/\Phi_1^2 \text{ (at } \beta) - 1/\Phi_1^2 \text{ (at } \beta + \Delta\beta).$$

The sensitivity determined in this way increased linearly with Φ_1. Figure 11 shows that at $\Phi_1 = 25$ the percentage error in D is five times the error for $\Phi_1 = 5$, with the same percentage error in β. At any constant value of β, sensitivity is high for small values of Φ_1, and decreases with increasing Φ_1.

V. CONCLUSIONS

It has been demonstrated that up to 255°C, the true mechanism for the deuterium–neopentane exchange is a single-step exchange in which the hydrogen

atoms of the hydride molecules exchange with deuterium atoms, one at a time. When this reaction takes place in a single porous catalyst particle consisting of reduced palladium on silica-alumina, the multistep kinetics can be explained by a model which imposes intraparticle mass transfer and desorption limitation on the surface exchange reaction. The product distribution for this reaction can be represented by two parameters: β, the ratio of exchange rate to desorption rate, and Φ_1, the Thiele modulus. Results of kinetic experiments, where various catalyst pretreatments and catalyst size reductions were employed, have provided evidence that β and Φ_1 are independent parameters and each represent a different transport process.

Thiele diffusion coefficients obtained by kinetic experiments have been shown to be about one-half of those obtained by Wicke–Kallenbach experiments. This difference may be partly the result of pore size distributions in the catalysts, as larger pores have more influence on the Wicke–Kallenbach diffusivity, and smaller pores have more influence on the Thiele diffusivity. Literature values of the Wicke–Kallenbach diffusivity may be twice as large as the Thiele diffusivity, the correct one to use in catalysis.

ACKNOWLEDGMENT

Acknowledgment is made to the Donors of the Petroleum Research Fund, administered by the American Chemical Society, for the support of this research.

REFERENCES

1. Wei, J., and Prater, C. D., *in* "Advances in Catalysis" (D. D. Eley, P. W. Selwood and P. B. Weisz, Eds.), Vol. 13, p. 203. Academic Press, New York, 1962.
2. Wei, J., *J. Catal.* **1**, 526 (1962).
3. Wei, J., *J. Catal.* **1**, 538 (1962).
4. Mikovsky, R. J., and Wei, J., *Chem. Eng. Sci.* **18**, 253 (1963).
5. Kemball, C., *Trans. Faraday Soc.* **50**, 1344 (1954)
6. Bolder, H., Dallinga, G., and Kloosterziel, H., *J. Catal.* **3**, 312 (1964).
7. Dwyer, F. G., Eagleton, L. C., Wei, J., and Zahner, J. C., *Proc. Roy. Soc., Ser. A* **302**, 253 (1968).
8. Dwyer, F. G., PhD thesis, Chem. Eng. Dep., Univ. of Pennsylvania, 1966.
9. Wicke, E., and Kallenbach, R., *Kolloid Z.*, **97**, 135 (1941).
10. Weisz, P. B., and Prater, C. D., *in* "Advances in Catalysis" (W. G. Frankenburg, V. I. Komarewsky and P. B. Weisz, Eds.), Vol. 6, 143 (1954).
11. Balder, J. R., and Petersen, E. E., *J. Catal.* **11**, 195, 202 (1968).
12. Stoll, D. R., and Brown, L. F., *J. Catal.* **32**, 37 (1974).
13. Wakao, N., Kimura, H., and Shibata, M., *J. Chem. Eng. Jap.* **2**, 51 (1969).
14. Omata, H., and Brown, L. F., *AIChE J.* **18**, 967 (1972).
15. Horak, Z., and Schneider, P., *Chem. Eng. J.* **2**, 26 (1971).
16. Wakao, N., and Smith, J. M., *Chem. Eng. Sci.* **17**, 825 (1962).
17. Johnson, M. F. L., and Stewart, W. E., *J. Catal.* **4**, 248, (1965).
18. Rothfeld, L. B., *AIChE J.* **9**, 19 (1963).
19. Scott D. S., and Dullien, F. A. L., *AIChE J.* **8**, 113 (1962).
20. Weisz, P. B., and Schwartz, A. B., *J. Catal.* **1**, 399 (1962).
21. Satterfield, C. N., "Mass Transfer in Heterogeneous Catalysis." M.I.T. Press, Cambridge, MA, 1970.
22. Huggill, J. A. W., *Proc. Roy. Soc., Ser. A* **212**, 123 (1952).
23. Lund, L. M., and Berman, A. S., *J. Chem. Phys.* **28**, 363 (1958).
24. Hanley, H. J. M., and Steele, W. A., *J. Phys. Chem.* **68**, 3087 (1964).
25. Ernst, W. R., PhD dissertation. Chem. Eng. Dep., Univ. of Delaware, 1974.
26. Hashimoto, K., and Silveston, P. L., *AIChE J.* **19**, 368 (1973).
27. Dwyer, F. G., Lago, R. M., Wei, J., and Zahner, J. C., at *Int. Congr. Catal., 4th, 1968* Pap. 8.
28. Weisz, P. B., *Z. Phys. Chem., Neue Folge* **11**, 1 (1957).